JOURNAL OF SPACECRAFT AND ROCKETS
Vol. 35, No. 6, November–December 1998

Arcing on Aluminum Anodized Plates Immersed in Low-Density Plasmas

B. V. Vayner,* C. V. Doreswamy,† D. C. Ferguson,‡ J. T. Galofaro,§ and D. B. Snyder§
NASA Lewis Research Center, Cleveland, Ohio 44135

A number of experiments have been done to study characteristics of the plasma contamination and electromagnetic radiation generated by arcing on anodized aluminum plates immersed in low-density plasma. The low-Earth-orbit plasma environment was simulated in a plasma vacuum chamber, where the parameters could be controlled precisely. Diagnostic equipment included two antennas, a mass spectrometer, a spherical langmuir probe, a wire probe, and a very sensitive current probe to measure arc current. All data except for mass spectrometry were obtained in digital form with a sampling interval of 2.5 ns that allowed us to study the radiation spectrum at frequencies up to 200 MHz. We found that the level of interference considerably exceeds the limitations on the level of electromagnetic noise set by technical requirements on Space Shuttle operation. Experiments with two independently biased plates have shown that the arcing onset on one plate generates a pulse of current on the second plate and that the secondary current pulse has a significant amplitude. The sampling interval for mass spectrometry was 250 ms. This allowed us to obtain the rate of plasma contamination due to arcing. A significant degradation of the coating layer was determined by measurement of the resistance of the plate, which had experienced a few hundred arcs.

Nomenclature

A = atomic number
a = diameter of hole in the shield, m
C = capacitance, F
D = langmuir probe diameter, m
D_h = diameter of damaged area, m
d = thickness of coating layer, m
E = electrical field strength, V/m
e = electron charge, C
F = flux of atoms, atoms/m^{2}s
f = frequency, Hz
f_e = plasma frequency, Hz
I_m = amplitude of discharge current, A
L = distance between plates, m
l = antenna length, m
M = atomic mass, kg
N_e = number of electrons
N_i = number of ions
n_e = electron number density, m^{-3}
p = neutral gas pressure, torr
Q = electrical charge, C
R = resistance, Ω
T_e = electron temperature, eV
t = time, s
t_d = time delay, s
U = bias voltage, V
U_a = amplitude of antenna voltage, V
V_p = plasma expansion speed, m/s
δ = skin depth, m
ρ = coating material density, kg/m^3
τ = pulse duration, s

Received Jan. 28, 1998; revision received May 20, 1998; accepted for publication May 25, 1998.

*Senior Research Associate, Ohio Aerospace Institute, Photovoltaic and Space Environment Effects Branch. E-mail: vayner@lerc.nasa.gov. Member AIAA.

†Visiting Researcher, Photovoltaic and Space Environment Effects Branch; currently Professor, Tuskegee University, Tuskegee, AL 36088.

‡Senior Scientist, Photovoltaic and Space Environment Effects Branch. Member AIAA.

§Physicist, Photovoltaic and Space Environment Effects Branch.

Introduction

ANY spacecraft being placed in Earth orbit or moving to the outer planets interacts with the space plasma. A wide range of these interactions has been studied for years,[1–7] but space systems become more complex, grow in dimensions, transfer huge amounts of information, and need much more powerful energy supplies. All of this demands detailed and profound research in the field. Among the many aspects of the problem, there is one that is of particular interest: arcing on spacecraft surfaces with a high-negative potential and its consequences. It is quite obvious that arcs are undesirable events, and the main purpose of current research is to elaborate methods for arc mitigation.[8–10] However, previous experience shows that electrical discharges occur on the surfaces of a high-voltage solar array, between two conductors with different potentials, and between spacecraft thermally insulated surfaces and the surrounding plasma. Moreover, the deployment of such large spacecraft as the International Space Station (ISS) in low Earth orbit (LEO) will create additional conditions stimulating the onset of arcing due to the use of high-voltage solar arrays, frequent docking and extravehicular activities, and complicated structures with insulated and conducted surfaces exposed to the plasma. Even though special measures have been adopted to control floating potentials (such as the plasma contactor), no one can guarantee an absolute prevention of arcing.[11]

Arcing onset is a stochastic process. Arcs occur randomly on spacecraft surfaces, and it is impossible to predict the moment and site of arcing. However, it is possible to determine the most probable sites of arcing and to prevent the adverse consequences by implementing a special procedure that must be followed. An ideal tool for designers might consist of the following blocks of computer programs: 1) to compute the distribution of the electrostatic potentials for given parameters of orbit, spacecraft geometry, and space weather; 2) to determine the most dangerous sites by implementation of well-known dependencies of arc rate on plasma density, electron temperature, surface material, and voltage; and 3) to adjust the design for arc mitigation. The greater part of blocks 1) and 2) exists now. The NASCAP code can be used for the computations of potentials,[12] and the results of the statistical analysis of large arrays of experimental data can be employed to determine zones having the highest probability for arcing onset.[13–16] There are also some new results concerning arc mitigation on solar arrays that could be useful for design adjustment. Nonetheless, even one arc may destroy sensitive electronics and/or generate disturbances in radio signal transmission. Arcs damage thermal insulation and contaminate surrounding plasma and scientific instruments. To prevent such negative consequences of arcing at the design stage, it seems necessary

to determine the spectra and absolute levels of electromagnetic radiation generated by arcing [electromagnetic interference (EMI)], magnitudes, and pulse forms of arc current and to investigate the influence of arcs on other spacecraft surfaces situated near the arc site.

A number of ground and space experiments have been done during the last decade to determine the arc rate and threshold, the magnitude and duration of current pulse, and the spectrum and intensity of EMI.[17–20] Undoubtedly, space experiments have some advantages: Equipment operates in the natural plasma environment during many days or even months, and both short-time and long-time processes caused by interactions with the plasma can be analyzed. But there are always strong limitations on the volume and kind of data that may be collected due to technical requirements for experimental devices installed on spacecraft. On the contrary, ground experiments have the advantage of a controlled environment and an unlimited choice of measurements that may be done. Many different tests have been performed in a space plasma simulation chamber.[21] High-quality data were obtained regarding EMI and plasma waves generated by arcs,[22,23] and the expansion of the plasma cloud was also investigated.[24] In spite of this long time and fruitful activity, the following issues need more profound investigation: the level and spectrum of EMI, the influence of arcs on the nearest spacecraft surfaces biased to high-negative potentials, and the degree of degradation of thermal insulation caused by arcing. In the present paper we describe the results of experimental study and theoretical analysis that were carried out to elucidate these problems.

Experimental Setup

All of our experiments were performed in large vacuum tanks (1.8-m diam and 3-m length) installed at the NASA Lewis Research Center. Vacuum equipment provided pressures as low as 10^{-7} torr. Two Penning sources generated an argon (or xenon) plasma with the electron density $n_e = (2\text{–}10)10^5$ cm^{-3}, temperature $T_e = 1\text{–}1.2$ eV, and neutral gas pressure $p = (0.8\text{–}7)10^{-5}$ torr, which were steady during the experiment. An anodized aluminum plate (18×18 cm) was mounted vertically at the bottom of the chamber, and it was biased by a high-voltage power supply through the resistor $R = 100$ kΩ. At the first stage of the experiment, we studied electromagnetic radiation, and diagnostic equipment included two spherical langmuir probes each with diameter $D = 1.9$ cm, two perpendicular antennas each with length $l = 56$ cm, and two wire probes (Fig. 1). For the second stage of the experiment, two pairs of plates were installed with separations of $L = 25$ and 50 cm, respectively, and each plate was biased by an independent power supply. The back sides and edges of plates were insulated by Kapton® films. Because the plates themselves have a low capacitance, additional capacitors, $C = 0.22\ \mu$F (0.47 μF for some experiments), were installed between the plates and ground. These capacitors allowed us to increase the electrical charge collected on the plates to more adequately simulate the real situation on spacecraft. The setup provided the possibility to investigate the influence of an arc initiated on one plate on the processes that were going on on the second plate. The circuit diagram of the experiment is shown in Fig. 2. All data were obtained in digital form with the sampling interval 2.5 ns. Thus,

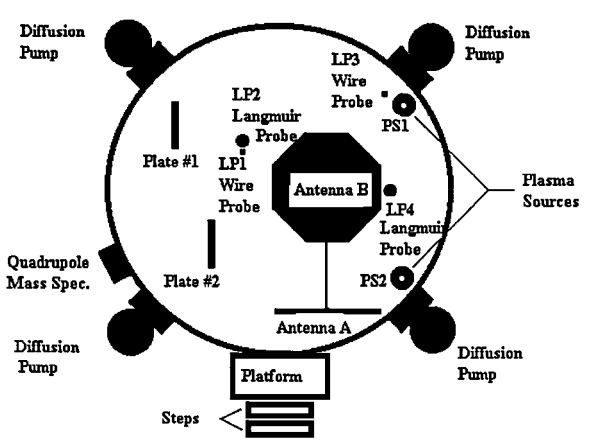

Fig. 1 Vertical chamber; dimensions: 1.8 × 3.0 m.

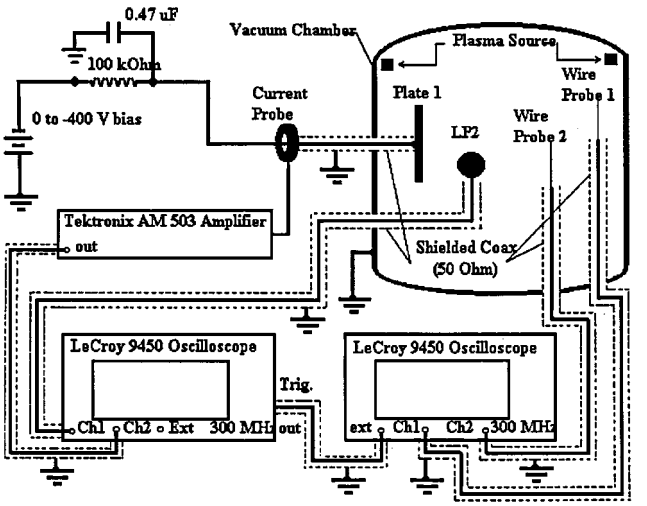

Fig. 2 Experimental setup for ground tests.

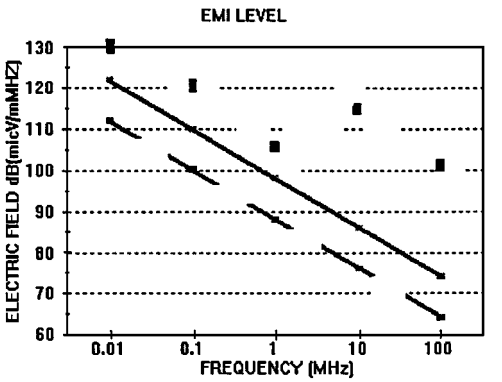

Fig. 3 Upper limits on EMI for the Shuttle: ——, payload in payload bay; – – –, equipment on flight deck (Ref. 19); and ■■■, EMI from arcs at ≈1-m distance.

we are able to study electromagnetic oscillations with frequencies up to 200 MHz. At the third stage of the experiment, the anodized aluminum plate (12×12 cm) was mounted in the vacuum chamber at the distance of 30 cm, facing the window of a mass spectrometer. This plate was biased to high negative voltage (−300 V) to provide an arc rate of 0.3–0.5 arcs/s. Aluminum atoms ejected from the arc sites were registered by the mass spectrometer with the sampling interval 250 ms. As a result of these measurements, we obtained the rate of plasma contamination and thermal coating degradation caused by arcing.

Experimental Results

High-Frequency EMI

It is now well established that the most probable sites for arcing onset are the cells of solar arrays with high-negative potentials and anodized aluminum surfaces exposed to the space plasma.[25,26] Arc discharge current generates both plasma waves and electromagnetic radiation, which can disturb the operation of electronics. The experimental study of plasma waves has shown that the most intense waves are langmuir waves with frequencies up to 20 MHz for LEO conditions.[23] The measured electrical field strength $E \approx 0.1$ V/m · MHz could be considered quite significant at distances of a few meters from the arcing site, and these measurements confirmed the necessity of shielding sensitive electronics. High-frequency transverse electromagnetic waves occupy a wide range on the frequency scale (results are obtained for $f \leq 200$ MHz), and their magnitudes are quite large even though the spectra demonstrate a drop of approximately 20 dB/decade (Refs. 22 and 23). The EMI field strength depends on the bias voltage, decreasing by 40 dB when the voltage decreases from 1 kV to 250 V. One can see from the results of our measurements (Fig. 3) that the registered level of radiation greatly exceeds the level of radiofrequency noise allowed for the Space Shuttle.[27] Theoretical calculations and

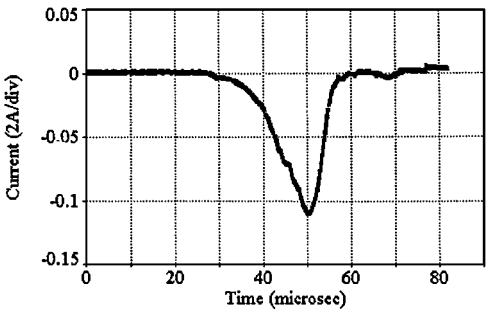

Fig. 4 Typical current pulse waveform measured during experiments with one plate, 18 × 18 cm, additional capacitance $C = 0.22$ μF, and bias voltage $U = -250$ V.

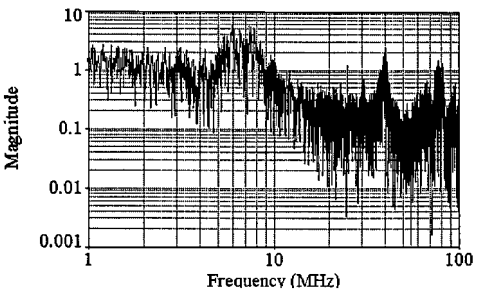

Fig. 5a Spectrum (mV/MHz) of the signal on antenna B.

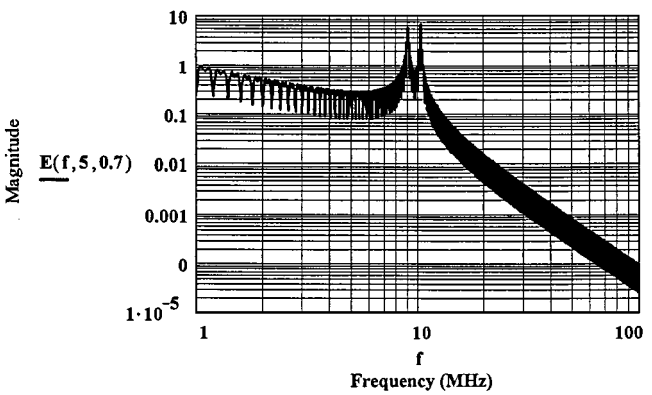

Fig. 5b Theoretical spectrum for the plasma density $n_e = 10^6$ cm^{-3} and the electron temperature $T_e = 1.2$ eV.

computer simulations have shown that both the amplitude and spectrum of EMI depend on the arc current parameters.[23,28,29] A typical current pulse wave form is shown in Fig. 4. Large space structures (for example, ISS) have a high electrical capacitance (a few microfarads) that results in a large stored electrical charge, and as a consequence, high-amplitude discharge currents I_m and comparably long pulse durations τ. Previous measurements[22] of EMI were done with an additional capacitance $C = 2000$ pF that seems not to adequately simulate the real situation. This is one of the reasons that we performed a number of experiments with insulated antennas and additional capacitors of 0.22 and 0.47 μF. Moreover, as has been observed, the high-frequency part of EMI spectrum is determined by short-time fluctuations in the arc current.[23] This makes theoretical calculations of the real EMI spectrum impossible if one implements a simple pulse form approximation, as was suggested in Refs. 28 and 29. Our calculations have shown that the theoretical spectrum is in quite good agreement with the experiments at the frequencies $f < 10$ MHz, but the high-frequency part of spectrum cannot be simulated within the framework of the simple model (Fig. 5) (see Ref. 23 for details). The results of two experiments are shown in Fig. 6. For most of the measurements the amplitude of voltage in the horizontal antenna is almost equal to that in the vertical antenna (Fig. 6, left-hand panels). However, a few experiments demonstrated some difference between the amplitudes of signals on the two antennas (Fig. 6, right-hand panels). For this particular experiment, the electrical field strength can be estimated as

$$E \approx \frac{U_a}{l} = \begin{cases} 0.06\ \text{V/m vertical antenna} \\ 0.12\ \text{V/m horizontal antenna} \end{cases} \tag{1}$$

Both spectra have some common features: a broad peak at the plasma frequency f_e and an almost flat spectrum at frequencies $f > f_e$. Because all measurements were performed in the near-field zone, the attenuation of low-frequency waves ($f < f_e$) in the plasma was negligible. One can see from the spectra in Fig. 6 that the signals have peaks at frequencies $f_m \approx 1/\tau$, which are equal to 40–50 kHz for the current experiment. To consider the influence of EMI on electronic equipment, one should take into account the thickness of metal covering the equipment (because skin depth $\delta \propto 1/f$), the size of holes in the conducting shields (because the penetration factor is proportional to f^2a^2), and the operational bandwidth of the receiver that could be influenced. All of these problems are beyond the scope of our paper, but the results obtained can be used as a basis for the development of a computational tool for designers.

A few remarks should be added regarding the results of these experiments. First, the 10 consecutive measurements of arc current pulse forms and the response of both antennas demonstrate almost identical features. This observation allows us to suggest that the arc current direction is roughly perpendicular to the plate. Otherwise, we would have found a significant difference in the amplitude of voltage on the two antennas because the electrical field strength has the highest amplitude in the direction parallel to the direction of current flow. We attribute rarely observed differences to the events that occur near the edge of the plate.

The second remark concerns the spectrum of EMI. The installation of an additional capacitor increases the duration of the current pulse to $\tau = 20$–25 μs. Space experiments with samples of solar arrays have shown that the duration of pulses may be as short as 0.2–0.4 μs with the same amplitude 1–3 A (Refs. 20 and 23). In such a case, the spectrum has a maximum at frequencies of 2.5–5 MHz, and assuming the same slope of the spectral curve, we may expect a significant increase in the EMI intensity in the high-frequency part of the spectrum. On the other hand, the capacitance of a spacecraft can reach tens of microfarads, which means only the short-time oscillations in the arc current contribute to the high-frequency EMI.

Plasma Effects from Arcing

The amount of electrical charge injected into the plasma during the arc pulse can be estimated from the measurement of current (Fig. 4)

$$Q \approx I_m \cdot \tau \tag{2}$$

This value depends on the capacitance, and it is equal to 50–100 μC for all of our experiments (for more details, see Ref. 23). Another estimate is not so confirmative but is very informative. Namely, the electrical charge stored on the plate before an arc is equal to

$$Q' = C \cdot U \tag{3}$$

The magnitude of Q' lies in the range 50–120 μC, depending on the additional capacitance. This value is in quite good agreement with the estimate obtained from Eq. (2), taking into account the relation between stored and lost charges $Q = (0.5$–$0.8)\,Q'$ (Ref. 24). It seems convenient to express the value of the injected electrical charge as the number of electrons

$$N_e = Q/e = 6 \times 10^{12}\,Q \tag{4}$$

This number of charged particles ($\sim 10^{14}$) increases the plasma density in the tank considerably.

One more estimate for the number of ions injected into the plasma can be made from the measurement of the size of the arc trace on the plate. Black spots of destroyed aluminum oxide coating with diameters $D_h = 0.2$–0.3 mm were observed, which means that the number of injected ions is equal to

$$N_i = \frac{\pi \cdot D_h^2}{4} \cdot d \cdot \frac{\rho}{M} \approx 10^{15} \tag{5}$$

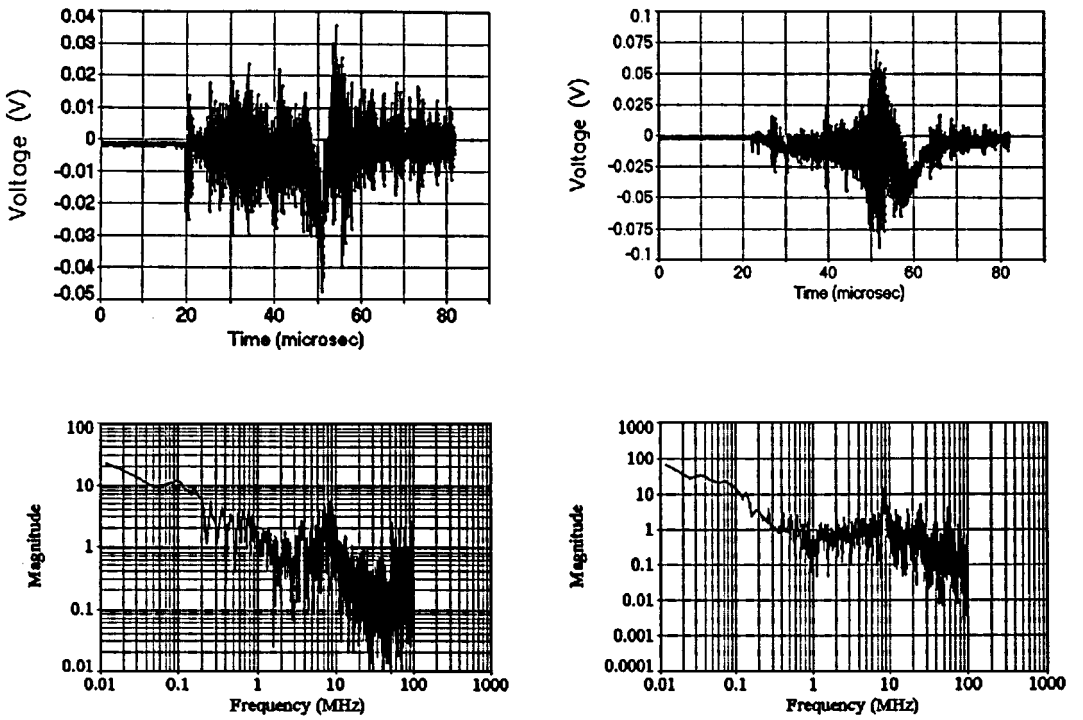

a) Horizontal

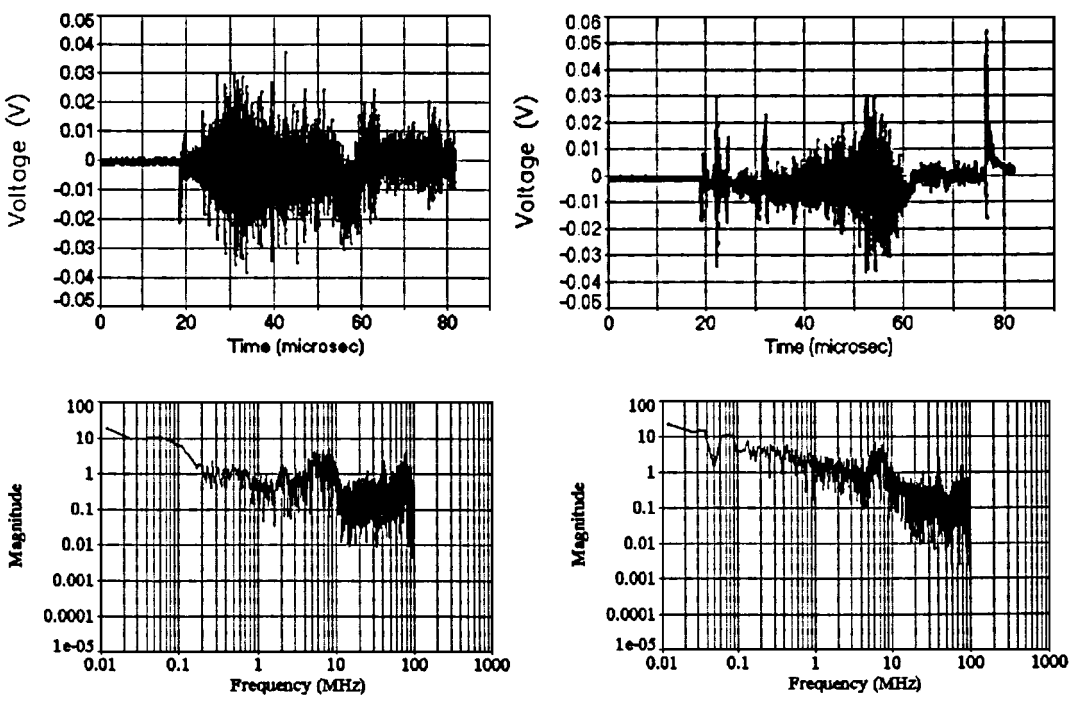

b) Vertical

Fig. 6 Signals and their spectra registered by two perpendicular antennas.

With such a sharp increase in the number of charged particles in the tank, we may expect some kinds of secondary effects on the independently biased plate mounted near the plate where arc occurs. Our first series of experiments was done with plates mounted at a separation of $L = 25$ cm, facing each other. When breakdown on the first plate occurs, the capacitor discharges through the plasma, and a current probe registers a pulse of current (Fig. 7a). A positive charge accumulated on the dielectric surface is in the process of being rapidly neutralized by plasma electrons, and the plasma potential changes abruptly. The potential difference between the plasma and the second plate decreases: This means a positive current pulse has to be registered by the second current probe. After some delay ($\sim 10\ \mu$s), an expanding plasma cloud reaches the second plate, which is biased at a lower negative voltage. In this case, the second current probe is expected to measure a current pulse with positive amplitude again. In fact, two different oscillograms were obtained from the experiment. In the first case, the second probe registered a low-amplitude positive current pulse, as was expected (Fig. 7b). One can see in Fig. 7b that a small peak of negative current is observed simultaneously with the arc pulse on the first plate. We suggest that a fast change in the electrical field strength due to breakdown is responsible for this peak. An expected time interval between pulses can be evaluated as

$$t_d \approx L / V_p \tag{6}$$

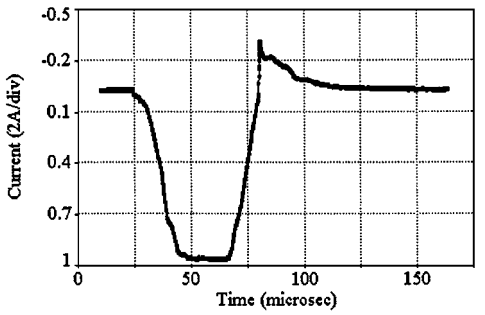

a) $U = -300$ V

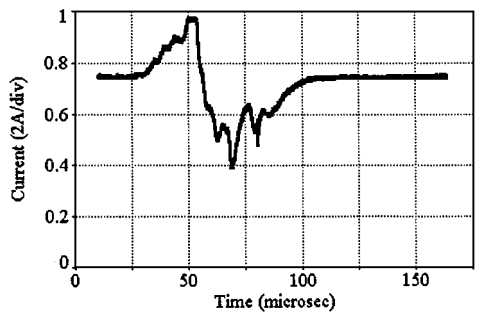

b) $U = -250$ V

Fig. 7 Arc current pulses registered on two independently biased plates.

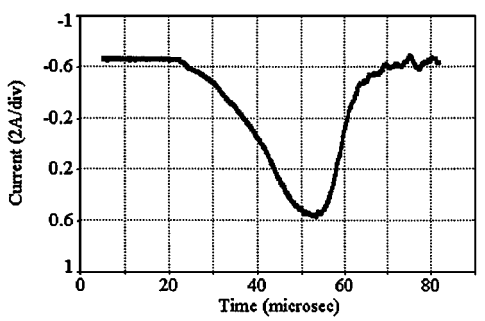

Fig. 8a Arc current pulse form to provide timescale for experiment shown in Fig. 8b.

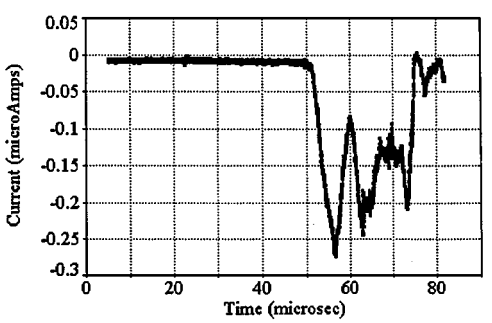

Fig. 8b Two-peak pulse structure registered by the wire probe mounted 50 cm from the plate.

We did observe a time delay of 8–10 μs, which confirms the earlier result obtained in Ref. 24: $V_p = 25$–30 km/s. A two-peak structure was also registered by a wire probe mounted 50 cm from the plate (Fig. 8). The significant increase in plasma density due to arcing had already been established by computing the spectrogram of the plasma waves.[23] All of these results can be explained within the framework of the simple physical model discussed earlier.

However, during a few experiments we observed an effect that could be called induced arcing[30] (Fig. 9). It is seen from the graphs that an arc on the first plate generates a negative pulse of current on the second plate, and both amplitudes are comparable. This kind of event cannot be explained until further experimental work will be

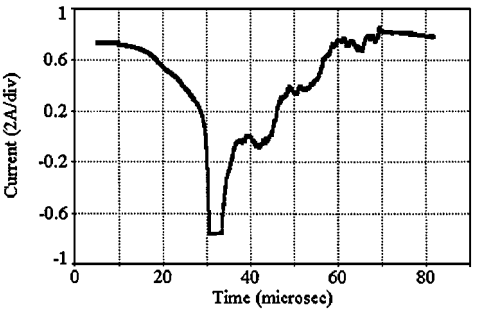

Fig. 9a Arc occurs on the plate biased − 300 V.

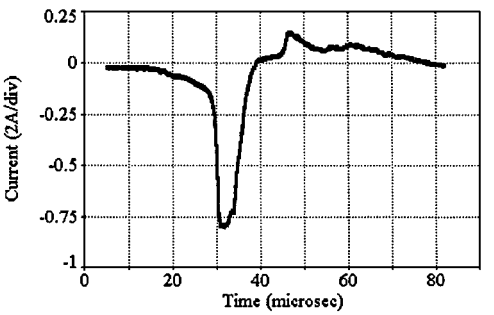

Fig. 9b Current probe registers pulse of current on the second plate biased − 250 V.

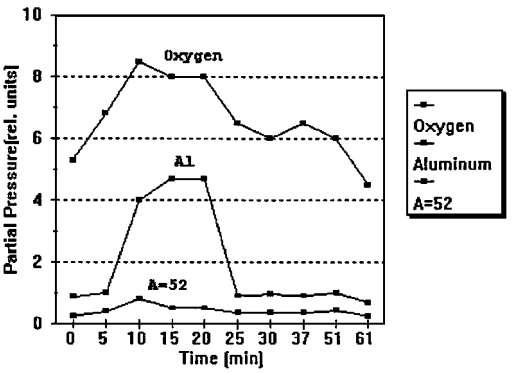

Fig. 10 Increase in abundance of aluminum, oxygen, and heavy atoms caused by arcing, which begins at $t = 0$ and ends at $t = 20$ min.

done. An important result of our experiment is the measurement of the current pulse on the second plate. In all variants we conclude that a negatively biased surface situated a few decimeters from the arcing site undergoes significant potential changes. This could mean a considerable current pulse in an electric circuit, for instance, in solar array connectors.

Plasma Contamination and Surface Degradation

To determine plasma contamination, we mounted the aluminum anodized plate (12×12 cm size and $d = 2.5$ μm) at a distance of 30 cm facing the window of the mass spectrometer. The back side and edges of the plate were insulated by the Kapton strips. The plate was biased negatively 300 V to provide the arc rate of 15 arcs/min, and additional capacitor with the capacitance $C = 1$ μF was installed between plate and ground to supply enough energy for each arc. The initial pressure for this particular experiment was as low as 0.5 μtorr, and xenon plasma was generated with the neutral gas pressure $p = 8$ μtorr, electron temperature $T_e = 1.2$ eV, and electron number density $n_e = 10^6$ cm^{-3}. The plate had been biased for 20 min, and data from the mass spectrometer were registered at 5-min intervals. The temporal behavior of plasma contamination is shown in Fig. 10. We believe that the observed peaks in concentrations of atoms with atomic masses $A = 27$ and 16 can be explained by the ejection of aluminum and oxygen during the arcing. We also observed an increase in concentration for atoms with the atomic mass $A = 52$, but we could not identify this element. Theoretical calculations have

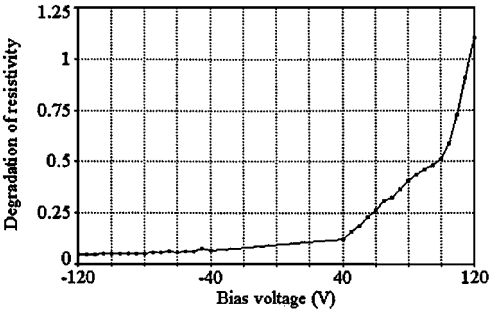

Fig. 11 Ratio of the final resistivity to the initial resistivity of the anodized layer vs bias voltage.

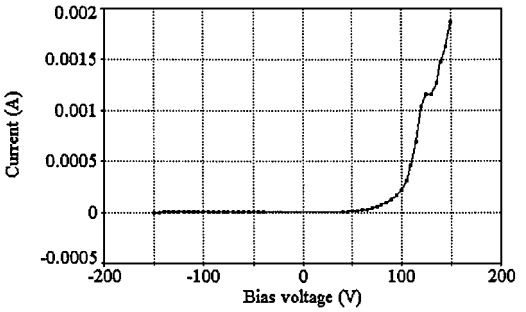

a) Virgin anodized plate

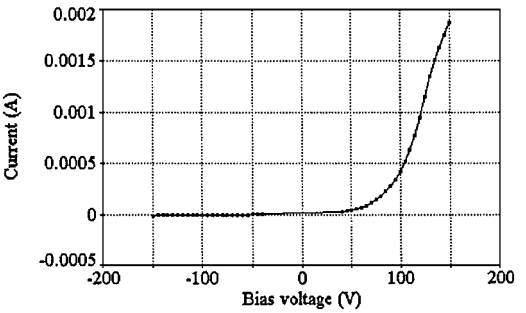

b) Plate having undergone 600 arcs

Fig. 12 Current–voltage curve.

shown that this rate of contamination corresponds to an average flux of aluminum atoms, $F = 10^8$ atoms/m^{2}s. The flux is very low, and we may conclude that arcs cannot contaminate special optical surfaces mounted at the distances above a few decimeters from the arc site.

To determine the degradation of thermal insulation, we have measured an electrical resistivity of the coating layer. The decrease in resistivity caused by 600 arcs is shown in Fig. 11. It is seen that the resistivity had fallen by a factor of 10. The exponential growth that is measured for bias voltages $U > 50$ V can be caused by snapover on the anodized aluminum plate. The events of snapover were observed many times in the ground and space experiments.[31,32] This effect is important because the collection current increases dramatically when the potential of the insulated surface reaches a threshold. For the particular case under investigation, this threshold is as low as 50 V, although snapover threshold is believed to be above 120 V for solar arrays.[32] Current–voltage characteristic curves are shown in Fig. 12 for the virgin plate and the plate having undergone 600 arcs. Inception of snapover at $U = 50$ V is clearly seen. One can see that the threshold does not change, but the collection current is higher for the plate having experienced arcing.

Conclusion

It is well known that arcing on spacecraft surfaces is an unavoidable event with adverse consequences. An extensive experimental and theoretical study of arcing onset and its aftermath has been carried out with the purpose of obtaining the quantitative characteristics of these physical processes. As a result of our efforts we have data regarding the arc rate dependence on the bias voltage and space environment parameters, the intensity and spectrum of the EMI, the degree of plasma contamination and thermal insulation degradation, and some other effects on the conductive surfaces situated near the arcing site. We believe that incorporation of the collected results in well-elaborated computer codes for calculations of the electrostatic field distribution along the spacecraft (NASCAP and EWB) can provide an effective tool for designers. The realization of this program will greatly increase the reliability of spacecraft operation.

References

[1]Stevens, N. J., "Space Environment Interactions with Spacecraft Surfaces," NASA TM-79016, 1979.

[2]Ferguson, D. C., "Interactions Between Spacecraft and Their Environment," NASA TM-106115, 1993.

[3]Martin, A. R., "A Review of Spacecraft/Plasma Interactions and Effects on Space Systems," *Journal of the British Interplanetary Society*, Vol. 47, No. 2, 1994, pp. 134–142.

[4]Bond, R. A., Pearce, A. J., and Martin, A. R., "Space Plasma Interactions with High Voltage Solar Arrays and Large Structures," *Journal of the British Interplanetary Society*, Vol. 47, No. 2, 1994, pp. 143–150.

[5]Hastings, D. E., "A Review of Plasma Interactions with Spacecraft in Low Earth Orbit," *Journal of Geophysical Research*, Vol. 100, No. A8, 1995, pp. 14,457–14,483.

[6]Tribble, A.C., *The Space Environment: Implications for Spacecraft Design*, Princeton Univ. Press, Princeton, NJ, 1995.

[7]Hastings, D., and Garrett, H., *Spacecraft-Environment Interactions*, Cambridge Univ. Press, New York, 1996.

[8]Ferguson, D. C., "Environmental Interactions and the SP-100 Power System," NASA TM-105866, 1993.

[9]Upschulte, B. L., Marinelli, W. J., Carleton, K. L., Weyl, G., Aifer, E., and Hastings, D. E., "Arcing of Negatively Biased Solar Cells in a Plasma Environment," *Journal of Spacecraft and Rockets*, Vol. 31, No. 3, 1994, pp. 493–501.

[10]Mong, R., and Hastings, D. E., "Arc Mitigation on High Voltage Solar Arrays," *Journal of Spacecraft and Rockets*, Vol. 31, No. 4, 1994, pp. 684–690.

[11]Ferguson, D. C., Snyder, D. B., and Carruth, R., "Findings of the Joint Workshop on Evaluation of Impacts of Space Station Freedom Ground Configurations," NASA TM-103717, 1990.

[12]Mandell, M. J., Jongeward, G. A., and Cooke, D. L., "Spacecraft–Plasma Interaction Codes: NASCAP/GEO, NASCAP/LEO, POLAR, DynaPAC, and EPSAT," *Proceedings of the Fifth Annual Workshop on Space Operations Applications and Research (SOAR'91)* (Houston, TX), Vol. 2, NASA Conf. Publication 3127, 1991, pp. 672–679.

[13]Ferguson, D. C., "The Voltage Threshold for Arcing for Solar Cells in LEO-Flight and Ground Test Results," AIAA Paper 86-0362, Jan. 1986.

[14]Ferguson, D. C., "Solar Array Arcing in Plasmas," *Proceedings of the 3rd Annual Workshop on Space Operations Automation and Robotics* (Houston, TX), NASA Conf. Publication 3059, 1989, pp. 509–513.

[15]Guidice, D. A., Curtis, H. B., Piszczor, M. F., and Palys, J. R., "Survey of Experimental Results from One Year of PASP Plus Orbital Operation," AIAA Paper 96-2331, July 1996.

[16]de la Cruz, C. P., Hastings, D. E., Ferguson, D., and Hillard, B., "Data Analysis and Model Comparison for Solar Array Module Plasma Interactions Experiment," *Journal of Spacecraft and Rockets*, Vol. 33, No. 3, 1996, pp. 438–446.

[17]Hastings, D. E., Weyl, G., and Kaufman, D., "Threshold Voltage for Arcing on Negatively Biased Solar Arrays," *Journal of Spacecraft and Rockets*, Vol. 27, No. 3, 1990, pp. 539–544.

[18]Hillard, G. B., and Ferguson, D. C., "Measured Rate of Arcing from an Anodized Sample on the SAMPIE Flight Experiment," AIAA Paper 95-0487, Jan. 1995.

[19]Leung, P., "Characterization of EMI Generated by the Discharge of a 'VOLT' Solar Array," Jet Propulsion Lab., Final Rept. JPL D-2644, California Inst. of Technology, Pasadena, CA, Oct. 1995.

[20]Vayner, B. V., and Ferguson, D. C., "Low-Frequency Waves in the Plasma Environment Around the Shuttle," *Journal of Spacecraft and Rockets*, Vol. 33, No. 2, 1996, pp. 255–261.

[21]Ferguson, D. C., "The Role of Space Plasma Simulation Chambers in Spacecraft Design and Testing," NASA Lewis Research Center, Rept. 96380, Feb. 1996.

[22]Leung, P., and Plamp, G., "Characteristics of RF Resulting From Dielectric Discharges," *IEEE Transactions in Nuclear Science*, No. 529, 1985, pp. 1610–1614.

[23]Vayner, B. V., Ferguson, D. C., Snyder, D. B., and Doreswamy, C. V., "Electromagnetic Radiation Generated by Arcing in Low Density Plasma," NASA TM-107217, 1996.

[24]Vaughn, J. A., Carruth, M. R., Jr., Katz, I., Mandell, M. J., and Jongeward, G. A., "Electrical Breakdown Currents on Large Spacecraft in Low

Earth Orbit," *Journal of Spacecraft and Rockets*, Vol. 31, No. 1, 1994, pp. 54–59.

[25]Cho, M., and Hastings, D. E., "Computer Particle Simulation of High-Voltage Solar Array Arcing Onset," *Journal of Spacecraft and Rockets*, Vol. 30, No. 2, 1993, pp. 189–201.

[26]Ferguson, D. C., and Hillard, G. B., "Preliminary Results from the Flight of the Solar Array Module Plasma Interactions Experiment (SAMPIE)," NASA Lewis Research Center, Internal Rept., 1995.

[27]NASA Johnson Space Center, Interface Control Document, ICD 2-19001, Houston, TX, 1989.

[28]Metz, R. N., "Radiating Dipole Model of Interference Induced in Spacecraft Circuitry by Surface Discharges," NASA TP-2240, 1984.

[29]Damas, M. C., and Robiscoe, R. T., "Detection of Radio-Frequency Signals Emitted by an Arc Discharge," *Journal of Applied Physics*, Vol. 64, No. 2, 1988, pp. 566–574.

[30]Doreswamy, C. V., Ferguson, D. C., Galofaro, J. T., Snyder, D. B., and Vayner, B. V., "A Comprehensive Study of Arcing on Aluminum Anodized Plates Immersed in Low Density Plasmas," *Proceedings of the International Conference on Phenomena in Ionized Gases* (Toulouse, France), Vol. 2, Université Paul Sabatier, Toulouse, France, 1997, pp. 146, 147.

[31]Davis, V., and Gardner, B., "Parasitic Current Collection by Solar Cells in LEO," AIAA Paper 95-0594, Jan. 1995.

[32]Ferguson, D., Hillard, G., Snyder, D., and Grier, N., "The Inception of Snapover on Solar Arrays: A Visualization Technique," AIAA Paper 98-1045, Jan. 1998.

A. C. Tribble
Associate Editor